

Entangling two defects via the surrounding crystal

T. Fogarty,¹ E. Kajari,² B. G. Taketani,² A. Wolf,² Th. Busch,¹ and G. Morigi^{2,3}

¹*Physics Department, University College Cork, Cork, Ireland*

²*Theoretische Physik, Universität des Saarlandes, D-66123 Saarbrücken, Germany*

³*Departament de Física, Universitat Autònoma de Barcelona, E-08193 Bellaterra, Spain*

(Dated: Wednesday 8th August, 2012)

We theoretically predict that two defects embedded in a crystalline structure, a harmonic chain, can be entangled through coupling with the crystal. Entanglement is found at long times for sufficiently cold chains and for a certain class of initial, separable states of the defects. The calculation is performed for a specific physical realization based on trapped ions, but can be extended to other systems exhibiting spatial order, such as optical lattices or cavity arrays in circuit QED. The predicted entanglement is robust against fluctuations of the chain parameters, such as its size, and of the elapsed time, as long as finite size effects can be neglected. Entanglement results from the interplay between localized modes in the regime in which the chain acts as a thermal bath for each individual defect, and is an example of quantum reservoir engineering.

PACS numbers: 03.67.Bg, 03.65.Yz, 42.50.Dv, 03.67.Mn

Entanglement is a quantum mechanical property, which has no classical counterpart. One of its peculiar features are the correlations of the measurement outcome between two entangled objects, even when they are at large distances [1]. These properties make entanglement a precious resource for quantum communication protocols and quantum metrology applications [2]. On the other hand, its quantum mechanical nature makes it fragile against coupling with the external world [3], especially when the spatial distance between the two objects is increased [4–6]. Understanding the dynamics of entanglement in open systems has recently become an active area of research focusing on thermalisation in quantum systems [7–10], and is awaiting experimental verifications.

Recently the idea has been put forward that the coupling with a reservoir can allow the robust preparation of a physical object in a nonclassical state and can permit its quantum coherent manipulation [11–14]. These concepts have been applied in order to create entangled states of matter [15], perform quantum simulations with trapped ions [16], and they are the basis for protocols for quantum networks [17, 18] and quantum metrology [19]. First analyses of the basic requirements for the onset of these dynamics, such as the properties of the system-bath coupling, have recently been performed [20–26]. Conditions for observing entanglement in optomechanical and biological systems are also being discussed [24, 26].

In Refs. [27, 28] some of the current authors investigated a paradigmatic model in which two defects couple to a linear chain of oscillators. Generic conditions were identified under which entanglement can be established between the defects via the common reservoir, which otherwise would lead to thermalization of a single defect [29].

In this Letter we build on these ideas and show that the capability to tune the frequency of the system (the defects) in a non-Markovian reservoir allows one to generate entanglement between remote systems, even when

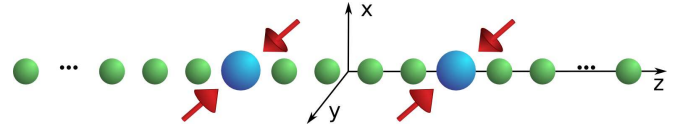


FIG. 1: (Color online) Two defects of larger mass are embedded into a linear chain of ions. A laser standing wave illuminates the defect ions and couples their transverse and axial displacements via the mechanical effects of light. For a certain class of initial separable states, the defects transverse motion becomes entangled by the coupling with the axial phonons of the chain.

the reservoir acts as a thermal bath in the presence of a single defect. Memory effects are due to the presence of the second defect, so that entanglement is generated by means of localized modes of the chain which involve the defects and is found for time scales over which the finite-size effects of the bulk can be neglected. Our discussion here focuses on a specific example, namely, a chain of trapped ions which includes two ions of different species (see Fig. 1). Nevertheless, the dynamics we discuss are of general nature and can be encountered in systems such as dipolar gases in optical lattices [30, 31], optomechanical systems [24], and cavity arrays in circuit quantum electrodynamics [32]. We also mention that a proposal for generating entanglement in a chain of 3 ions using laser cooling has been discussed in Ref. [33]. In this Letter we identify a mechanism, that allows one to generate entanglement between two ions in a chain of any size, and which is solely generated by the coupling with the external environment. In a specific limit, the dynamics discussed here reproduce the predictions in [33].

We consider a chain of ions of charge Q and mass m , that is aligned along the z axis and contains two defect ions, as sketched in Fig. 1. The defects have same charge Q but mass $M > m$ and are assumed to

be trapped sufficiently far away from the chain edges. The chain is stabilized by a linear Paul trap, whose effective potential is described by the secular potential $V_{\text{trap}}(\mathbf{r}_j) = (U_{\parallel} z_j^2 + U_{\perp,j}(x_j^2 + y_j^2))/2$. Here, $j = 1, \dots, N$ labels the ions along the chain, $\mathbf{r}_j = (x_j, y_j, z_j)$ denotes their positions, and U_{\parallel} and $U_{\perp,j} = (U_0/m_j - U_{\parallel})/2$ determine the strength of the axial and transverse potentials. Here the mass dependence of $U_{\perp,j}$ is due to the radio-frequency potential which creates the transverse confinement [34]. This property, which is specific to ion traps, implies that the defects transverse motion is a localized oscillation in the chain for sufficiently large mass ratios M/m [35].

The ions are assumed to have been laser cooled to a temperature T such that they perform harmonic vibrations about their respective equilibrium positions $\mathbf{r}_j^{(0)} = (0, 0, z_j^{(0)})$, which are determined by the balance of the trap force and the Coulomb repulsion. In the harmonic approximation, axial and transverse excitations are decoupled and the dynamics is governed by the quadratic Hamiltonian $H_0 = H_{\parallel} + H_{\perp}^{(x)} + H_{\perp}^{(y)}$, with

$$H_{\parallel} = \sum_{j=1}^N \left(\frac{p_{j,z}^2}{2m_j} + \frac{1}{2} U_{\parallel} q_j^2 + \frac{1}{4} \sum_{\ell \neq j} \mathcal{K}_{j,\ell} (q_j - q_{\ell})^2 \right), \quad (1)$$

$$H_{\perp}^{(x)} = \sum_{j=1}^N \left(\frac{p_{j,x}^2}{2m_j} + \frac{1}{2} U_{\perp,j} x_j^2 - \frac{1}{8} \sum_{\ell \neq j} \mathcal{K}_{j,\ell} (x_j - x_{\ell})^2 \right), \quad (2)$$

and $q_j = z_j - z_j^{(0)}$. Here, $p_{j,\alpha}$ is the $\alpha = x, y, z$ component of the momentum \mathbf{p}_j of ion j and $\mathcal{K}_{j,\ell} = 2Q^2/|z_j^{(0)} - z_{\ell}^{(0)}|^3$ is the coupling due to the Coulomb repulsion [36]. The Hamiltonian term $H_{\perp}^{(y)}$ is found from $H_{\perp}^{(x)}$ by replacing $x_j \rightarrow y_j$. We denote the location of the defect ions by $j = j_1, j_2$ and assume that $m_{j_1} = m_{j_2} = M$. The mutual distance between the ions is chosen to be small compared to the chain length, $j_2 - j_1 \ll N$ and we require $1 \ll j_1 < j_2 \ll N$.

Let us first analyze the spectrum of the Hamiltonian H_0 . For simplicity, we assume equally-spaced axial equilibrium positions with constant interparticle distance $a = z_{j+1}^{(0)} - z_j^{(0)}$. Such a situation can be realised in optical lattices and exists in the central region of long ion chains [37] and in anharmonic axial potentials [38]. Fig. 2(a) displays the spectra of the axial and transverse modes for the specific case of $M \approx 2.87m$, which corresponds to In^+ ions embedded in a Ca^+ chain [39]. We find two degenerate normal mode frequencies for each transverse spectrum, stemming from the localized vibrations at the positions of the defects, which are separate from the respective transverse branch. If the frequency gap between localized modes and the transverse branch is sufficiently large, these modes coincide approximately with the defects transverse vibrations. In this limit the

defects transverse modes are strongly coupled with each other via the Coulomb interaction, and weakly coupled to the rest of the chain [40].

Using the isolated frequencies and the long-range Coulomb interaction, entanglement between the two transverse modes of the defects can be generated by preparing each mode in a squeezed state and letting the dynamics evolve: the defects will become entangled in the same way a beam splitter entangles two optical modes which are prepared in a squeezed state [41]. We assume that the chain is initially in a thermal state at temperature T while the initial state of the transverse modes are identical separable squeezed vacuum states along the x direction with variances $\Delta x_{j_1,j_2}^2 = x_0^2 e^{2s}/2$ and $\Delta p_{j_1,j_2}^2 = p_0^2 e^{-2s}/2$. Here $x_0 = \sqrt{M/U_{\parallel}}$ is the size of the defect ground state in the axial potential, $p_0 = \hbar/x_0$ is the associated momentum, and s is the real-valued squeezing parameter [41]. The defects' state remains Gaussian under the evolution described by the quadratic Hamiltonian, Eq.(2), and is hence fully characterized by the first moments $\langle \xi_j \rangle$ and the covariance matrix $\Sigma_{ij} = \frac{1}{2} \langle \xi_i \xi_j + \xi_j \xi_i \rangle - \langle \xi_i \rangle \langle \xi_j \rangle$, where $\xi = (x_{j_1}/x_0, p_{x,j_1}/p_0, x_{j_2}/x_0, p_{x,j_2}/p_0)$ [42]. Entanglement between the defect modes can then be quantified by means of the logarithmic negativity, $E_N = \max\{0, -\ln(2\tilde{\nu}_-)\}$, where $\tilde{\nu}_-$ is the smallest symplectic eigenvalue of the partial transpose of the covariance matrix Σ [43, 44]. Figure 2(b) displays E_N as a function of time when the defects are at a distance $d = 7a$ for initial squeezing of $s = 0, 0.5$. One can see that E_N grows as a function of time and increases as s is increased (see grey curves). Surprisingly we also find entanglement for $s = 0$, which can be explained by the fact that the defects are not eigenmodes of the transverse spectrum. Numerical simulations show that this entanglement decreases as the mutual distance between the defects is increased and it can therefore be understood as a consequence of the form of the transverse eigenmodes.

We will now demonstrate that entanglement between the defects can be generated and substantially enhanced by coupling the defect modes to the axial phonons of the chain. For this purpose we consider an interaction which couples the defects' transverse displacements with the corresponding axial displacements. The chain dynamics is then given by the Hamiltonian $H = H_0 + H_I(t)$, where

$$H_I(t) = \frac{\gamma(t)}{2} [(x_{j_1} - q_{j_1})^2 + (x_{j_2} - q_{j_2})^2], \quad (3)$$

with $\gamma(t) = \gamma \Theta(t)$ being an effective coupling strength and $\Theta(t)$ the Heaviside function. This coupling could be realized, for instance, using a standing-wave laser field in the $x - z$ plane, resonant with an optical transition of the defect ions, and which has nodes at their equilibrium positions. The Lamb-Dicke regime is also assumed. At $t > 0$ a displacement of each defect along x excites a wave

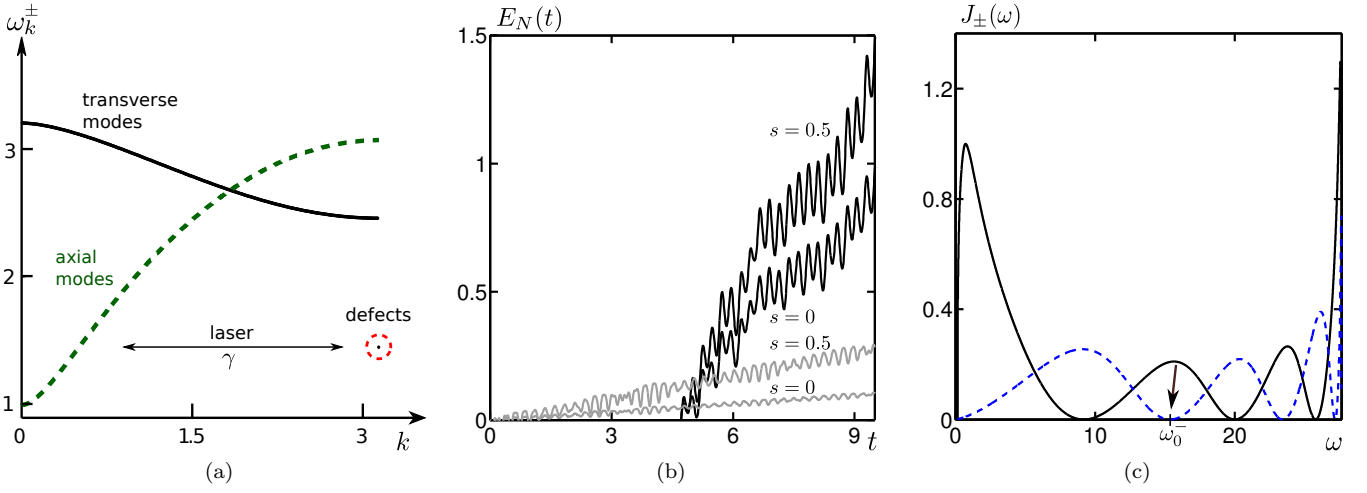


FIG. 2: (Color online) Results for two In^+ ions embedded in a chain of 50 Ca^+ ions with a mutual distance of $d = 7a$. The mass ratio is $M/m = 2.87$ [39]. (a) (Doubly-degenerate) eigenfrequencies ω_k of H_\perp (solid) and H_\parallel (dashed line) as a function of the quasimomentum k (in units of π/a). The frequencies are in units of $\omega_\parallel = \sqrt{U_\parallel/m}$. The parameters are $U_\perp(m)/U_\parallel = 2000$ and $\omega_\parallel = 2\pi \times 26.1\text{kHz}$. The isolated transverse frequencies (see dashed circle) almost coincide with the frequency of the defects transverse potential. (b) Logarithmic negativity as a function of time t , in units of ω_\parallel^{-1} . Black (grey) curves represent the case with laser coupling switched on (off), with coupling strength $\gamma = 18.2m\omega_\parallel^2$. Labels indicate the initial squeezing of the defects vibrations, while the rest of the chain is initially prepared at $T = 8\hbar\omega_\parallel/k_B$ (here: $T = 10\mu\text{K}$). (c) Spectral density, in units of $m\omega_\parallel^2$, as a function of the frequency, in units of ω_\parallel . The solid (dashed) line correspond to $J_+(\omega)$ ($J_-(\omega)$). The arrow indicates the transverse trap frequency of the defects chosen for the solid curves in (b) [46].

packet of quasi-resonant axial phononic modes (note that displacements along y are decoupled and will be ignored from now on). In the following we numerically evaluate the defects' dynamics, starting from the formal solution of the coupled Heisenberg equations of transverse, axial, and defect modes of Hamiltonian H .

Let us, without loss of generality, consider a simplified situation, where the defects are symmetrically placed with respect to the trap center and where the Hamiltonian (2) is therefore invariant under the exchange of the j -th and the $(N - j + 1)$ -th ion ($j \in \{1, \dots, N/2\}$). By performing a change of coordinates, $q_j^\pm = (q_{N-j+1} \pm q_j)/\sqrt{2}$ and $X_\pm = (x_{j1} \pm x_{j2})/\sqrt{2}$, one can immediately see that the defects' transverse center-of-mass (COM) displacement, X_+ , couples to the axial displacements q_j^+ , and the same holds for X_- and q_j^- . The action of the axial vibrations on the dynamics of the defects' collective variable can be characterized in terms of the corresponding spectral densities $J_\pm(\omega) = \sum_{k=1}^{N/2} \pi(\gamma_k^\pm)^2/(2m\omega_k^\pm)\delta(\omega - \omega_k^\pm)$, where γ_k^\pm is the coupling strength of the coordinate X_\pm to the k -th normal mode of the corresponding axial reservoir with eigenfrequency $\omega_k^\pm \equiv \omega_k$ [27, 45]. Fig. 2(c) displays the spectral densities $J_\pm(\omega)$ for $d = 7a$. The appearance of frequency values $\omega_k^\pm = \omega_\ell^\pm$, at which either the spectral density J_+ or J_- vanishes, is a signature of the coupling between the defects and the excitations of the ions between them. This can give rise to localized exci-

tations when the frequencies of the defects can be tuned to coincide with one of the zeros, which we denote by $\omega_0^- \equiv \omega_\ell^- \simeq \sqrt{U_\perp(M)/M}$ [46]. Under these conditions, one generates a decoherence free subspace for the relative motion of the defects, corresponding to an eigenmode involving the defects and the ions of the chain localized between them. Entanglement between the defects can thus be generated for an initial state in which both are in a squeezed state while the rest of the chain is in a thermal state. In fact, the dynamics leads to thermalization of the defects' COM motion, X_+ , and destroys all initial correlations between the defects' COM and relative motion, while the relative coordinate preserves part of the initial squeezing. Sufficiently large initial squeezing and low initial temperature can therefore lead to two-mode squeezing of the defects' transverse motion [28, 47], and therefore to entanglement [48]. We note that, while this argument is based on reflection symmetry in the chain about the center, such symmetry is irrelevant as long as the distance of the defects from the edges of the chain is large and their mutual distance is much smaller than the chain size. In this limit, our model is valid for any positioning of the defects, for time scales over which finite-size effects can be neglected.

The solid curves in Fig. 2(b) show the entanglement created in a chain of $N = 50$ ions, with a coupling strength of $\gamma = 18.2m\omega_\parallel^2$ and two initial values for the squeezing. The curves are shown for times over which

finite-size effects can be neglected. Entanglement is built up after a transient time and reaches values which are about an order of magnitude larger than the values found in the absence of the coupling laser. Larger entanglement is found again by increasing the initial squeezing and also decreasing the temperature of the chain (not shown). Let us remark that, while cooling a large chain to ultralow temperatures is a challenging task, the basic requirement for observing the dynamics predicted here is that the axial mode of the chain resonant with the defect frequency is prepared in the ground state. In a chain of trapped ions this could be realized, for example, by cooling the motion of the defect ions while the laser coupling transverse and axial displacement is switched on [49]. For systems of ultracold gases this should not be a critical requirement, considering that the temperatures are of the order of few μK . We also notice that noise will not significantly affect the predicted dynamics, provided the chain eigenmode couples only weakly to the environment. If, for instance, the zero of the spectral density corresponds to an eigenmode with short wave wavelength, it will only be weakly heated by processes such as patch potentials at the electrodes of ion traps[50]. Entanglement between the defects will therefore be observable as long as the axial mode of the chain, corresponding to the zero of the spectral density, is cold and protected from external noise sources.

We finally demonstrate that the generation of entanglement is not a finite-size effect, and can indeed be found in chains of increasing size. Fig. 3 displays the logarithmic negativity as a function of time for various chain sizes and a mutual distance of $d = 15a$ between the defects. Here we assume that the COM motion is decoupled by tuning its frequency to a value at which the corresponding spectral density vanishes (see inset). The curves are displayed for times that are shorter than the revival time and have been rescaled by the size-dependent frequency $\omega_{\parallel} = \omega_{\text{ref}}\sqrt{\log N}/N$, where ω_{ref} is a constant and the size dependent factor corresponds to a scaling where the interparticle distance is kept constant in the center of a linear Paul trap. For this thermodynamic limit, the excitation spectrum of the chain is well defined [36]. One observes that the logarithmic negativity oscillates about a (quasi) stationary state, whose value is independent of the chain size. For increasing chain sizes the time window over which this entanglement is found also increases.

The resulting entanglement can be measured by extending the method developed in Ref. [51] to two Gaussian modes. The procedure consists of coupling the transverse oscillation of each defect with an ancillary qubit, such as an electronic transition of the defect ion. This can be done using the Hamiltonian $H_j^{\text{int}} = \hbar g_j(t) \sigma_j^z (a_j e^{-i\Omega_j t} + a_j^\dagger e^{i\Omega_j t})$, with $j \in \{j_1, j_2\}$ and where $a_j = (x_j/x_0 + ip_{x_j}/p_0)/\sqrt{2}$ annihilates a phonon of the defect transverse excitation

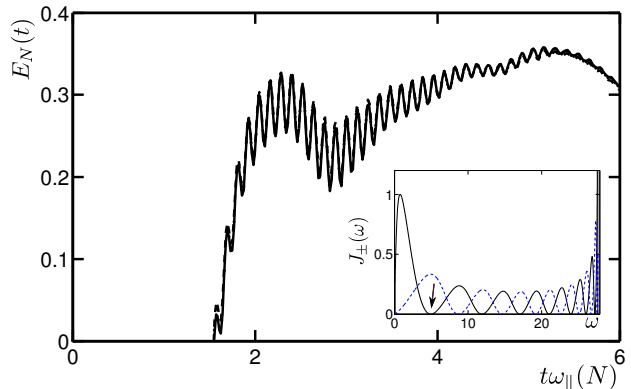


FIG. 3: (Color online) Logarithmic negativity as a function of time when $d = 15a$ for a chain with $N = 300$ (dashed), 500 (dotted) and 700 (solid line) ions (Note that all three curves are lying on top of each other). The chain temperature is $T = 0$, the defects' initial squeezing is $s = 0.5$. Time is in units of ω_{\parallel}^{-1} , where $\omega_{\parallel} = \omega_{\text{ref}}\sqrt{\log N}/N$ and $\omega_{\text{ref}} = 2\pi \times 659.6$ kHz [36]. The other parameters are $M/m = 2.87$ and $\gamma = 0.043 m\omega_{\text{ref}}^2$. Inset: corresponding spectral densities, in units of $m\omega_{\parallel}^2$.

at frequency $\Omega_j = \sqrt{U_{\perp}(M)/M}$. The frequencies g_j denote the Rabi coupling with the internal transition and $\sigma_j^{x,y,z}$ are the Pauli operators. The expectation value $\langle T \rangle = \langle \sigma^x \otimes \sigma^x - \sigma^y \otimes \sigma^y + i\sigma^x \otimes \sigma^y + i\sigma^y \otimes \sigma^x \rangle$, gives the characteristic function $\chi(\beta_1, \beta_2)$ of a two-mode continuous variable system, where $\beta_{1,2} = 2i \int_0^t dt' g_{j_1, j_2}(t') e^{i\Omega_{j_1, j_2} t'}$. The reconstruction of the oscillators state and thus of its entanglement properties is hence granted by properly designed coupling profiles. Note that, as Gaussian states are fully described by their first and second order moments, it is sufficient to probe their characteristic function close to the phase-space origin.

In conclusion, we have shown that robust entanglement can be created between two systems coupled by an external environment and identified the basic requirements. These include the capability to tune the defect frequency across a region of the spectrum, which allows entanglement to be mediated by an eigenmode of the reservoir, which must be sufficiently cold and protected from external noise sources. We have shown that these predictions can be tested in an experimental setting, focussing on the specific case of trapped ions. Nevertheless, due to their generality these dynamics can also be observed in other physical systems, such as cavity arrays, circuit QED and optomechanical systems. Our study sheds new light on the dynamics of thermalization and the role of the reservoir in establishing quantum correlations, and contributes to applications for scalable quantum technological implementations.

The authors acknowledge discussions with C. Cormick, J. Brito, G. De Chiara, C. Kurz, and E. Lutz, and

support by the European Commission (IP AQUITE, STREP PICC), the German Research Foundation and the Irish Research Council through the Embark Initiative RS/2009/1082.

-
- [1] A. Einstein, B. Podolsky, and N. Rosen, *Phys. Rev.* **47**, 777 (1935).
 - [2] R. Horodecki, P. Horodecki, M. Horodecki, and K. Horodecki, *Rev. Mod. Phys.* **81**, 865 (2009).
 - [3] W. H. Zurek, *Rev. Mod. Phys.* **75**, 715 (2003).
 - [4] K. Audenaert, J. Eisert, M. B. Plenio, and R. F. Werner, *Phys. Rev. A* **66**, 042327 (2002).
 - [5] J. Anders, *Phys. Rev. A* **77**, 062102 (2008).
 - [6] T. Zell, F. Queisser, and R. Klesse, *Phys. Rev. Lett.* **102**, 160501 (2009).
 - [7] S. Popescu, A. J. Short, and A. Winter, *Nature Phys.* **2**, 754 (2006).
 - [8] S. Goldstein, J.L. Lebowitz, R. Tumulka, and N. Zanghi, *Phys. Rev. Lett.* **96**, 050403 (2006).
 - [9] M. Rigol, V. Dunjko, and M. Olshanii, *Nature* **452**, 854 (2008).
 - [10] A. Riera, C. Gogolin, and J. Eisert, *Phys. Rev. Lett.* **108**, 080402 (2012).
 - [11] S. Diehl, A. Micheli, A. Kantian, B. Kraus, H. P. Büchler, and P. Zoller, *Nat. Phys.* **4**, 878 (2008).
 - [12] F. Verstraete, M. M. Wolf, and J. I. Cirac, *Nat. Phys.* **5**, 633 (2009).
 - [13] S. Pielawa, L. Davidovich, D. Vitali, and G. Morigi, *Phys. Rev. A* **81**, 043802 (2010).
 - [14] C. A. Muschik, E. S. Polzik, and J. I. Cirac, *Phys. Rev. A* **83**, 052312 (2011).
 - [15] H. Krauter, C. A. Muschik, K. Jensen, W. Wasilewski, J. M. Petersen, J. I. Cirac, and E. S. Polzik, *Phys. Rev. Lett.* **107**, 080503 (2011).
 - [16] J. T. Barreiro, M. Müller, P. Schindler, D. Nigg, T. Monz, M. Chwalla, M. Hennrich, C. F. Roos, P. Zoller, and R. Blatt, *Nature* **470**, 486 (2011).
 - [17] F. Pastawski, L. Clemente, and J. I. Cirac, *Phys. Rev. A* **83**, 012304 (2011).
 - [18] K. G. H. Vollbrecht, C. A. Muschik, and J. I. Cirac, *Phys. Rev. Lett.* **107**, 120502 (2011).
 - [19] G. Goldstein, P. Cappellaro, J. R. Maze, J. S. Hodges, L. Jiang, A. S. Sørensen, and M. D. Lukin, *Phys. Rev. Lett.* **106**, 140502 (2011).
 - [20] D. A. Lidar, I. L. Chuang, and K. B. Whaley, *Phys. Rev. Lett.* **81**, 2594 (1998).
 - [21] M. M. Wolf, J. Eisert, T. S. Cubitt, and J. I. Cirac, *Phys. Rev. Lett.* **101**, 150402 (2008).
 - [22] H.-P. Breuer, E.-M. Laine, and J. Piilo, *Phys. Rev. Lett.* **103**, 210401 (2009).
 - [23] A. Rivas, S.F. Huelga, and M.B. Plenio, *Phys. Rev. Lett.* **105**, 050403 (2010).
 - [24] M. Ludwig, K. Hammerer, and F. Marquardt, *Phys. Rev. A* **82**, 012333 (2010).
 - [25] Bi-Heng Liu, Li Li, Yun-Feng Huang, Chuan-Feng Li, Guang-Can Guo, E.-M. Laine, H.-P. Breuer, J. Piilo, *Nature Physics* **7**, 931 (2011).
 - [26] S. F. Huelga, A. Rivas, and M. B. Plenio, *Phys. Rev. Lett.* **108**, 160402 (2012).
 - [27] A. Wolf, G. De Chiara, E. Kajari, E. Lutz, and G. Morigi, *Europhys. Lett.* **95**, 60008 (2011).
 - [28] E. Kajari, A. Wolf, E. Lutz, and G. Morigi, *Phys. Rev. A* **85**, 042318 (2012).
 - [29] R. J. Rubin, *Phys. Rev.* **131**, 964 (1963), and references therein.
 - [30] I. Bloch, J. Dalibard, and W. Zwerger, *Rev. Mod. Phys.* **80**, 885 (2008).
 - [31] T. Lahaye, C. Menotti, L. Santos, M. Lewenstein and T. Pfau, *Rep. Prog. Phys.* **72**, 126401 (2009).
 - [32] J. Koch, A. A. Houck, K. L. Hur, S. M. Girvin, *Phys. Rev. A* **82**, 043811 (2010).
 - [33] C. Cormick and J. P. Paz, *Phys. Rev. A* **81**, 022306 (2010).
 - [34] See for instance D. Kielpinski, B. E. King, C. J. Myatt, C. A. Sackett, Q. A. Turchette, W. M. Itano, C. Monroe, D. J. Wineland, and W. H. Zurek, *Phys. Rev. A* **61**, 032310 (2000), and references therein.
 - [35] Other realizations of this property can be implemented in different systems using their specific features.
 - [36] G. Morigi and S. Fishman, *Phys. Rev. Lett.* **93**, 170602 (2004); *Phys. Rev. E* **70**, 066141 (2004).
 - [37] D. H. E. Dubin, *Phys. Rev. E* **55**, 4017 (1997).
 - [38] G.-D. Lin, S.-L. Zhu, R. Islam, K. Kim, M.-S. Chang, S. Korenblit, C. Monroe, and L.-M. Duan, *Europhys. Lett.* **86**, 60004 (2009).
 - [39] K. Hayasaka, *Appl. Phys. B* **107**, 965 (2012).
 - [40] We also note that non-harmonic terms couple them with the axial spectrum. We discard this effect assuming that the chain is sufficiently cold.
 - [41] See for instance S. L. Braunstein and P. van Loock, *Rev. Mod. Phys.* **77**, 513 (2005), and references therein.
 - [42] G. Adesso and F. Illuminati, *J. Phys A* **40**, 7821 (2007).
 - [43] G. Vidal and R. F. Werner, *Phys. Rev. A* **65**, 032314 (2002).
 - [44] M. B. Plenio, *Phys. Rev. Lett.* **95**, 090503 (2005).
 - [45] U. Weiss, *Quantum Dissipative Systems*, 2nd ed. (World Scientific, Singapore, 1999).
 - [46] More precisely, the resonance condition is $(\omega_0^-)^2 = (U_{\parallel} + \gamma)/M$, see also [27, 28].
 - [47] J. P. Paz and A. J. Roncaglia, *Phys. Rev. Lett.* **100**, 220401 (2008).
 - [48] M. D. Reid, P. D. Drummond, W. P. Bowen, E. G. Cavalcanti, P. K. Lam, H. A. Bachor, U. L. Andersen and G. Leuchs, *Rev. Mod. Phys.* **81**, 1727 (2009).
 - [49] M. D. Barrett, B. DeMarco, T. Schaetz, V. Meyer, D. Leibfried, J. Britton, J. Chiaverini, W. M. Itano, B. Jelenković, J. D. Jost, C. Langer, T. Rosenband, and D. J. Wineland, *Phys. Rev. A* **68**, 042302 (2003).
 - [50] H. Häffner, C. Roos, and R. Blatt, *Phys. Rep.* **469**, 155 (2008).
 - [51] T. Tufarelli, M. S. Kim and S. Bose, *Phys. Rev. A* **83**, 062120 (2011).